

## Formation of Three-Dimensional Islands in Subcritical Layer Deposition in Stranski-Krastanow Growth

V. Shchukin,<sup>1,\*</sup> N. Ledentsov,<sup>1</sup> and S. Rouvimov<sup>2</sup>

<sup>1</sup>*VI Systems GmbH, Hardenbergstraße 7, Berlin D-10623, Germany and A. F. Ioffe Physical Technical Institute of the Russian Academy of Sciences, Politeknicheskaya 26, St. Petersburg 194021, Russia*

<sup>2</sup>*University of Notre Dame, 112 North Notre Dame Avenue, South Bend, Indiana 46556, USA*  
(Received 15 October 2012; revised manuscript received 8 March 2013; published 23 April 2013)

A new method for the formation of three-dimensional (3D) strained islands in lattice-mismatched ( $B$  on  $A$ ) heteroepitaxy is proposed. Once  $B$  forms a wetting layer of a subcritical thickness, material  $C$  is deposited, which is lattice matched to  $A$  and does not wet  $B$ . Then  $B$  and  $C$  phase separate forming local  $B$ -rich and  $C$ -rich domains on the surface. The thickness of  $B$ -rich domains thus exceeds locally that of the initial film of  $B$ , and 3D islands may form as it is demonstrated by modeled phase diagrams of the  $C/B/A$  system. We show that the growth of the subcritical InAs/GaAs(100) film followed by the deposition of AlAs results (i) in the formation of Al-rich and In-rich domains in the wetting layer, confirmed by chemically sensitive scanning transmission electron microscopy, and (ii) in the stimulated onset of 3D islands, as evidenced both by high resolution transmission electron microscopy and by a significant redshift of the photoluminescence spectrum, which is in agreement with the proposed model.

DOI: [10.1103/PhysRevLett.110.176101](https://doi.org/10.1103/PhysRevLett.110.176101)

PACS numbers: 68.65.-k, 81.16.Dn, 81.16.Rf

The spontaneous formation of coherently strained nanometer-scale islands of materials lattice mismatched to a substrate [1] attracts continuous interest due to the possibility to create defect-free semiconductor quantum dot (QD) heterostructures [2]. In the last decade, advanced studies have been focused on more complex aspects of nanostructure formation involving several physical effects occurring at the same time, e.g., the addition of a small amount of a third material acting as surfactant [3] or antisurfactant [4], the formation of QDs from phase-separating alloys [5], wetting [6] or nonwetting [7] on solid surfaces, and the interplay between wetting and elasticity [8]. This has allowed a deeper insight in the surface phenomena at nanoscale distances as well as created new tools for engineering chemical composition, shape, and electronic spectra of nanostructures widely employed in microelectronic and optoelectronic devices.

In this Letter, we consider a novel mechanism of QD formation based on an interplay of four basic phenomena: wetting, nonwetting, phase separation, and elastic interaction, significantly altering the Stranski-Krastanow (SK) growth mode. The conventional SK growth known for many semiconductor systems (e.g., InAs/GaAs or Ge/Si) implies the onset of three-dimensional (3D) coherent islands on top of the wetting layer (WL) of a critical thickness. This is followed by the growth of islands in size and thinning of the WL. During the postdeposition evolution, the material exchange between the islands and/or the islands and the WL may result in the islands of equilibrium size [9,10], or the island growth can be kinetically limited by the barriers for the formation of new atomic layers on the island facets [11]. If no limiting size occurs, larger islands ripen at the expense of smaller ones.

The critical WL thickness is of high importance due to its effect on the electronic spectrum and on the carrier transport towards the QDs. Furthermore, the overall amount of a strained material is crucial for coherency, especially for stacked QDs, and it would be extremely advantageous to reduce the thickness of the WL in favor of QDs. The critical WL thickness for a given system being nearly constant for a large variety of the growth conditions can be eventually reduced if a long growth interruption is applied [12] typically leading, due to ripening, to low density QDs and the onset of large defect-rich islands.

The new mechanism of QD formation is distinct from the conventional SK growth mode in the following way. Let a material  $B$  lattice mismatched to a substrate  $A$  be deposited below the critical thickness. Then, on top of the WL of  $B$  a third material  $C$  is deposited that *does not wet*  $B$ . To be specific, we bear in mind that both the thermodynamically and kinetically dominated formation of surface nanostructures is possible [13] depending on a system. Moreover, close-to-equilibrium behavior was observed in the size distribution of Ge/Si islands [14] as well as in a reversible change of density, lateral size, and height of InAs/GaAs islands upon temperature cycling [15] before capping by GaAs. To elucidate the new mechanism of QD formation we also seek a surface equilibrium of a  $C/B/A$  system. We focus on moderate temperatures and neglect alloying. Further, we consider  $C$  lattice matched to  $A$  and not contributing to the islands. Then the equilibrium state of the system may include strained islands of  $B$  and a flat layer composed of  $B$  and  $C$ . To address possible structures of such a flat layer we apply a two-level wetting model [16–18] to describe wetting or nonwetting interactions. Then the surface energy of a film of  $N$  monolayers (MLs) of  $B$  on  $A$  is

$$\gamma_{BA}^{\text{surf}} = \gamma_A^{\text{surf}} + \Phi_{BA}[1 - \exp(-N/\delta)]. \quad (1)$$

Here  $\delta$  is the range of interatomic forces and the wetting constant  $\Phi_{BA} = \gamma_B^{\text{surf}} + \gamma_{BA}^{\text{int}} - \gamma_A^{\text{surf}}$  accounts for the creation of a surface of  $B$ , of a  $B/A$  interface and vanishing of a surface of  $A$ . Wetting implies  $\Phi_{BA} < 0$ . We note that Eq. (1), referring to the continuum model, also fits well to the results of the atomic scale calculations, both by the tight-binding model [16] and first principle approaches [17,18]. Thus (1) applies also to deposition below 1 ML where the deposited material forms a specific surface reconstruction rather than a continuous film.

We extend (1) and apply it to a system of 3 materials, where  $M$  MLs of  $C$  are deposited on top of a film having  $N$  MLs of  $B$ . Assuming the range  $\delta$  equal to every pair of materials, the surface energy of a  $C/B/A$  sandwich is

$$\gamma_{C/B/A}^{\text{surf}} = \gamma_A^{\text{surf}} + \Phi_{BA}[1 - e^{-N/\delta}] + \Phi_{CA}[1 - e^{-M/\delta}] + (\Phi_{CB} - \Phi_{CA})[1 - e^{-N/\delta}][1 - e^{-M/\delta}], \quad (2)$$

where  $\Phi_{CA} = \gamma_C^{\text{surf}} + \gamma_{CA}^{\text{int}} - \gamma_A^{\text{surf}}$  and  $\Phi_{CB} = \gamma_C^{\text{surf}} + \gamma_{CB}^{\text{int}} - \gamma_B^{\text{surf}}$ . Further, we assume that Eq. (2), like Eq. (1), is valid also for sub- and near-monolayer depositions.

The nonwetting of  $C$  on  $B$  ( $\Phi_{CB} > 0$ ) may lead to the instability of a homogeneous sandwich against separation into domains with different thicknesses of  $B$  and  $C$ . As mass conservation holds, the stability criteria of a homogeneous system are similar to those of a ternary alloy [19]:

$$\frac{\partial^2 \gamma}{\partial M^2} > 0 \quad \text{and} \quad \left( \frac{\partial^2 \gamma}{\partial N^2} \right) \left( \frac{\partial^2 \gamma}{\partial M^2} \right) - \left( \frac{\partial^2 \gamma}{\partial N \partial M} \right)^2 > 0. \quad (3)$$

Since  $\Phi_{CB} > 0$  and under a realistic relation between interface energies,  $-\gamma_{BA}^{\text{int}} - \gamma_{CB}^{\text{int}} + \gamma_{CA}^{\text{int}} < 0$ , the surface energy (2) at any  $N$  and  $M$  does not meet at least one of two criteria (3). Then a homogeneous sandwich is unstable and, as the alloying related entropy is neglected, decomposes into domains of pure  $B$  and pure  $C$ .

To seek the equilibrium state of a  $C/B/A$  system consider  $N$  MLs of  $B$  distributed between  $N_1$  MLs of a WL,  $N_2$  MLs of the pyramidal-shape islands with a tilt angle of facets  $\vartheta_B$  and an equal size  $L$ , and  $(N - N_1 - N_2)$  MLs forming ripened islands of the same shape and  $L \rightarrow \infty$ .  $M$  MLs of  $C$  form a WL layer occupying the fraction  $\nu$  of the surface. Then the total energy

$$\begin{aligned} E_{\text{total}} = & (1 - \nu)\Phi_{BA}(1 - e^{-N_1/[(1-\nu)\delta]}) \\ & + \nu\Phi_{CA}(1 - e^{-M/(\nu\delta)}) - (N - N_1)\Delta E_{\text{elast}}^{\text{relax}} \\ & + E_0 N_2 \left[ -2 \left( \frac{L_0}{L} \right)^2 \ln \left( \frac{e^{1/2} L}{L_0} \right) \right. \\ & \left. + \frac{L_0}{L} + b N_2^{3/2} \left( \frac{L_0}{L} \right)^{3/2} \right] \end{aligned} \quad (4)$$

includes the surface energy of two WLs, the elastic relaxation energy, which is the same for finite and ripened islands, and the energy of the array of finite islands. The latter

includes [9] the energy of elastic stress relaxation at the edges, the surface energy term, and the dipole-dipole elastic repulsion between the islands.  $L_0$  is the characteristic length, and  $E_0$  is the characteristic energy set by the elastic stress relaxation energy of the edges of the island of size  $L_0$ . The coefficient  $\alpha = 6a \cot \vartheta_B (E_0 L_0)^{-1} (\Delta \Gamma_0 - \Phi_{BA} \{1 - e^{-N_1/[(1-\nu)\delta]}\})$ , where  $a$  is the monolayer thickness, the change of the surface energy due to island formation is written as a sum of the terms dependent and independent of the WL thickness, and  $\Delta \Gamma_0 = \gamma_B^{\text{facets}} / \cos \vartheta_B + \gamma_{BA}^{\text{int}} - \gamma_A^{\text{surf}} - p\varepsilon$  includes the contributions due to the formation of tilted facets and of an interface beneath the islands, to the vanishing of a surface of the WL of  $B$ , and to strain-induced renormalization of the surface energies.

Seeking the minimum of the energy (4) with respect to  $L$ ,  $N_2$ ,  $N_1$ , and  $\nu$  [20] gives the equilibrium morphology of the system. Let, first,  $C$  moderately wet  $A$  ( $\Phi_{CA} = -0.8|\Phi_{BA}|$ ). To focus on essential physics, we present, out of many possible variants, two main phase diagrams. Figure 1(a) refers to a system, where 3D islands of  $B$  having a finite size are energetically favorable. Structure I is a flat WL formed of domains of  $B$  and  $C$ . Structure II refers to coexisting WL of  $B$ , WL of  $C$  and coherent islands of  $B$ , and structure III contains both coherent and ripened islands of  $B$ . For a larger amount of  $C$ , the WL of  $B$  vanishes, and the system contains the WL of  $C$  and islands of  $B$ , which are either only coherent (structure IV) or both coherent and ripened (structure V). The boundary between structure I and structure II or IV represents the conditions for the onset of 3D islands of  $B$ .

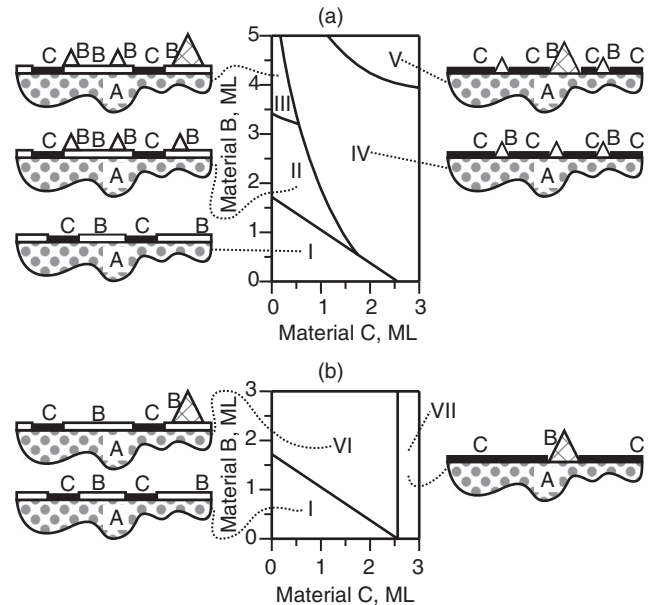


FIG. 1. Equilibrium phase diagrams of a  $C/B/A$  system. (a)  $B$  forms finite islands,  $\Delta \Gamma_0 = -72.2E_0$ . (b)  $B$  does not form finite islands,  $\Delta \Gamma_0 = -60E_0$ . Other parameters used are the same for (a) and (b):  $\Phi_{BA} = -87E_0$ ,  $\delta = 0.667$  ML,  $\Delta E_{\text{elast}}^{\text{relax}} = 10E_0$ ,  $\vartheta_B = 45^\circ$ ,  $L_0 = 53a$ , and  $\beta = 2.1$ .

Figure 1(b) refers to a system, where no finite size of 3D islands of  $B$  is energetically favorable, and a trend to ripening exists. Then the phase diagram, further to structure I, contains two others where ripened islands of  $B$  form either on the WL composed of domains of  $B$  and domains of  $C$  (structure VI) or on the WL of  $C$  (structure VII). We note that apart from the thermodynamic equilibrium, the actual kinetics in the system can strongly affect the resulting structure [21]. If, e.g., ripening is hindered by strain-induced barriers [11] resulting in 3D islands of a kinetically limited finite size, the boundary between structures I and VI refers again to the onset of 3D coherent islands of  $B$ . It follows from Figs. 1(a) and 1(b) that the adding of material  $C$  stimulates the onset of 3D islands of  $B$  at a subcritical deposition, i.e., at a smaller amount of  $B$  than in a  $B/A$  system, and this is a universal phenomenon, occurring for both thermodynamically controlled and kinetically controlled islands.

If  $C$  does not wet  $A$  ( $\Phi_{CA} > 0$ ) it is energetically favorable for material  $C$  to assemble in isolated droplets. The latter process can, however, be kinetically hindered. Let a film of material  $C$  from an area ( $D \times D$ ) and a thickness  $M$  MLs assemble in a droplet forming a droplet surface and reducing the surface of a flat WL. The energy change is then equal,  $\Delta E(D) = \tilde{\gamma}_{\text{droplet}}^{\text{surf}} (D^2 M a)^{2/3} - \Phi_{CA} D^2$ , where  $\tilde{\gamma}_{\text{droplet}}^{\text{surf}}$  is the effective surface energy of the droplet. The energy  $\Delta E(D)$  reveals a critical barrier of a height

$$W_{\text{cr}}^{\text{droplet}} = (4/27)(\tilde{\gamma}_{\text{droplet}}^{\text{surf}})^3 (M a)^2 \Phi_{CA}^{-2}. \quad (5)$$

Since the nonwetting of  $C$  on  $A$  is weaker than that of  $C$  on  $B$  ( $\Phi_{CA} < \Phi_{CB}$ ), the barrier for the formation of a droplet of  $C$  on the substrate  $A$  is significantly higher than the one for a droplet of  $C$  on the WL of  $B$ . Then the sandwich  $C/B/A$  can decompose rather fast forming  $B/A$  and  $C/A$  domains whereas further evolution of  $C/A$  domains to isolated droplets is kinetically hindered.

Although exact kinetics can be rather complex including, e.g., exchange reactions propelling atoms of  $B$  to the top and driving atoms of  $C$  on the substrate as well as effects on the atomic scale, the main trend is expected to persist: the strongest nonwetting interaction of  $C$  on  $B$  results in phase separation. The local thickness of the domains of  $B$  exceeds the nominal amount of the deposited  $B$  and thus provides an earlier onset of 3D islands of  $B$ .

AlAs/InAs/GaAs(100) is an example of a  $C/B/A$  system. For typical As-rich conditions, the As chemical potential  $\mu_{\text{As}} = \mu_{\text{As}}^{\text{bulk}} - 0.2 \text{ eV}$  and the surface reconstruction  $\beta 2(2 \times 4)$ , the surface energy of GaAs is  $\gamma_A = 58 \text{ meV}/\text{\AA}^2$ , the wetting constant InAs/GaAs is  $\Phi_{BA} = -14 \text{ meV}/\text{\AA}^2$  [17], and the surface energy of AlAs is  $\gamma_C = 68 \text{ meV}/\text{\AA}^2$  [22]. As interface energies for III-V materials are  $\sim 1 \text{ meV}/\text{\AA}^2$  [23], the wetting constants are governed mainly by the difference in surface energies. Thus, both AlAs/InAs and AlAs/GaAs are nonwetting, the wetting constants differ by a factor of 2.4, and the

heights of the barriers (5) differ by a factor of  $\sim 6$ . The effects of nonwetting can drive phase separation for AlAs on InAs and be kinetically hindered for AlAs on GaAs.

The proposed mechanism was verified by a deposition of 0.5 ML AlAs on subcritical WL (1.5 ML) of InAs/GaAs by molecular beam epitaxy using a multiwafer industrial molecular beam epitaxy reactor at  $480^\circ \text{C}$  substrate temperature and an As overpressure of  $\sim 2 \times 10^6$  Torr and a capping of the structure by GaAs. Single-sheet, threefold, and fourfold stacks with 2.5-nm GaAs spacers were grown. Figure 2(a) shows the cross-sectional high-angle annular dark-field (HAADF) image of the fourfold stack sample taken with the Ångström-size probe in scanning transmission electron microscopy (STEM). As HAADF contrast is sensitive to the atomic number ( $Z$  contrast, or chemically sensitive contrast), one sees an excess amount of Al (dark contrast) and In (bright contrast). Figure 2(b) shows scans of the vertical chemical profile taken at two different positions in the lateral plane by energy-dispersive x-ray spectroscopy. Apart from the AlAs marker above the stack, local maxima in Al concentration may occur at the layers where AlAs was deposited. A comparison of two scans shows that in each layer containing AlAs, a local maximum

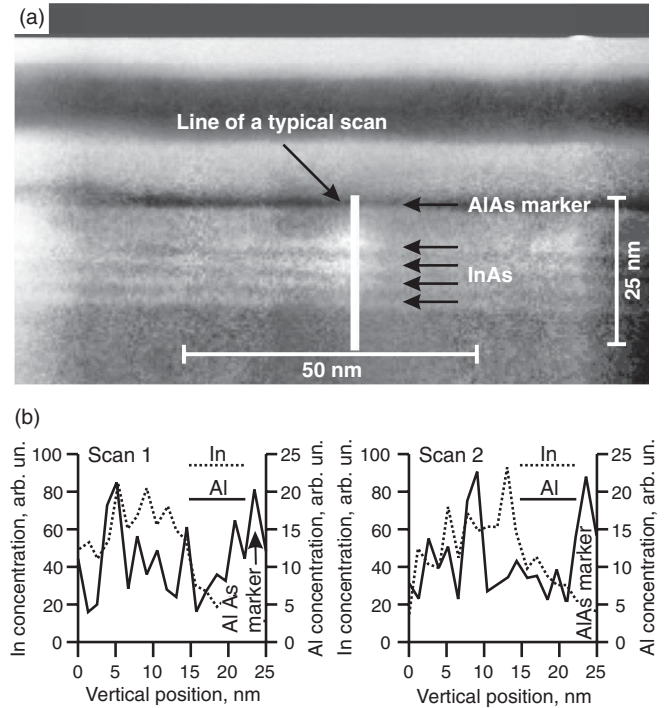


FIG. 2. (a) Cross-sectional high-angle annular dark-field scanning transmission electron microscopy image of a fourfold stack of AlAs/InAs/GaAs structures sensitive to atomic number ( $Z$  contrast). Bright contrast is In, dark contrast is Al, a thick layer on top is an AlAs marker. (b) Two vertical scans at different positions show that, for each layer of deposited InAs/AlAs, the concentration of Al drastically varies from scan to scan, which confirms the formation of Al-rich and Al-poor domains in the wetting layers.

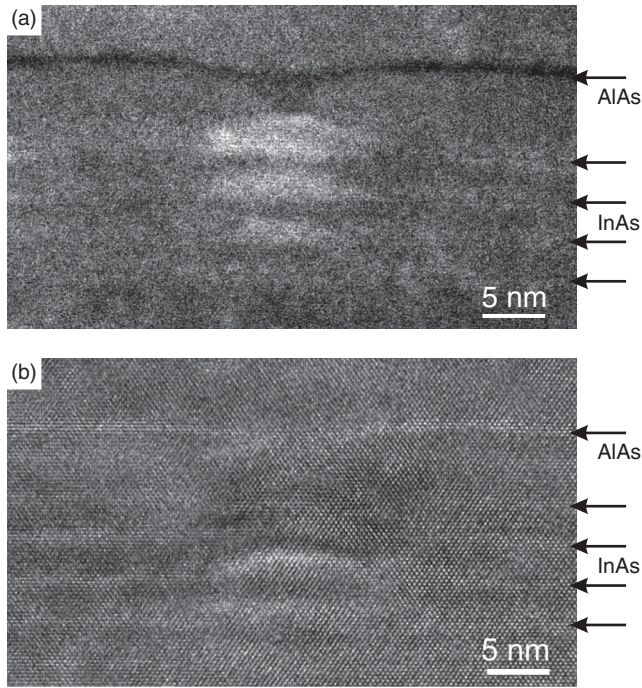


FIG. 3. Cross-sectional images of fourfold stacked islands. (a) High-angle annular dark-field scanning transmission electron microscopy image (chemically-sensitive contrast). (b) High resolution transmission electron microscopy (HRTEM) image.

of Al concentration is observed either in scan 1, or in scan 2, or in neither. This confirms the formation of Al-rich and Al-poor domains in each WL, according to the proposed model (see also Ref. [24]).

Figure 3(a) shows a cross-sectional HAADF STEM image as in Fig. 2(a), but at a larger magnification adjusted for a single stack of islands. Figure 3(b) is a cross-sectional HRTEM image of a fourfold stack.

Further, the onset of 3D islands manifests itself also in photoluminescence (PL) spectra [Figs. 4(a) and 4(b)]. The reference structures with only InAs deposited on GaAs reveal PL peaks at 0.85–0.95  $\mu\text{m}$  before [Fig. 4(b), filled squares] and at 1.05–1.2  $\mu\text{m}$  after the onset of 3D SK QDs. The deposition of 1.5 ML of InAs on GaAs followed by the deposition of 0.5 ML AlAs results in the PL peak at 1.08  $\mu\text{m}$  (filled circle). All structures are capped by GaAs without growth interruptions. Repeating the InAs-AlAs deposition 3 times using a 2.5-nm-thick GaAs spacer shifts the PL peak to  $\sim 1.23$   $\mu\text{m}$  (filled triangle). The width of the QD PL spectrum is comparable to that for conventional InAs/GaAs QDs used in device applications evidencing comparable size and shape uniformity.

We note that the phase separation of InAs and AlAs is indeed driven by the effects of nonwetting since the resulting structure depends on the sequence of the deposition (AlAs/InAs or *vice versa*) [25]. Similar effects were observed when 1 nm of AlAs was deposited after the formation of 3D SK InAs/GaAs QDs [26] resulting in a redshift of the PL peak up to 1.3  $\mu\text{m}$  and the vanishing of

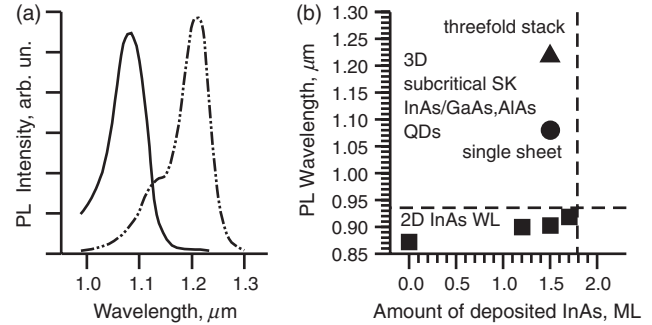


FIG. 4. (a) PL spectra at room temperature ( $\sim 1$  W/cm<sup>2</sup>, 532 nm) of the samples with a single sheet of InAs (solid line) and threefold stack of InAs with 2.5-nm GaAs spacers (dash-dotted line). The quantum dots are formed by subcritical InAs deposition (1.5 ML) followed by 0.5 ML AlAs deposition and GaAs overgrowth. (b) Spectral position of the PL peak in the InAs/GaAs system with and without a deposition of 0.5 ML AlAs. The deposition of AlAs on subcritical InAs/GaAs results in a significant redshift of the PL peak.

the InAs WL. Also, stimulated formation of InAs islands was reported for submonolayer InAs deposition and stacking with GaAs/AlGaAs spacers [27]. In case InAs and AlAs are deposited on GaAs together, both the effects of promoting and hindering of 3D InAs-rich islands are present, and the island formation should be less pronounced than that for subsequent depositions AlAs/InAs/GaAs [28].

To conclude, we considered a subcritical layer deposition of a wetting material  $B$  in a lattice-mismatched system  $B/A$  where the formation of 3D islands of  $B$  is stimulated, due to nonwetting phenomena, by adding a third material  $C$ . This may represent a fairly general approach to the QD growth as the mechanism applies if  $C$  moderately wets  $A$  or if  $C$  does not wet  $A$ , if there exists a finite equilibrium size of 3D islands of  $B$  or if the islands tend to ripen. Experimental studies of a subcritical InAs/GaAs system with 0.5 ML of deposited AlAs by STEM confirm the formation of Al-rich and Al-poor domains in the WL. The cross-sectional STEM and HRTEM images and a redshift of the PL spectrum reveal stimulated 3D islands forming QDs. Vertical stacking of coherent QDs is realized to reach the spectral range not accessible for InGaAs/GaAs quantum wells. This mechanism is expected also for other materials with similar wetting or nonwetting interactions, e.g., in the In-Ga-Al-N system.

We acknowledge support by the EU FP7 program under Agreement No. 318338 and the PIANO+ Collaborative R&D program (project SEPIANet).

\*vitaly.shchukin@v-i-systems.com

- [1] M. Zinke-Allmang, *Thin Solid Films* **346**, 1 (1999); P. Politi, G. Grenet, A. Marty, A. Ponchet, and J. Villain, *Phys. Rep.* **324**, 271 (2000); D.E. Jesson, in *Silicon Germanium and SiGe:Carbon*, edited by E. Kasper and

- K. Lyutovich, EMIS Datareviews Series, No. 24 (INSPEC, IEE, London, 2000), Chap. 1.1, p. 3; C. Teichert, *Phys. Rep.* **365**, 335 (2002); J. Stangl, V. Holy, G. Bauer, and C. B. Murray, *Rev. Mod. Phys.* **76**, 725 (2004).
- [2] D. Bimberg, M. Grundmann, and N.N. Ledentsov, *Quantum Dot Heterostructures* (John Wiley and Sons, Chichester, 1998); V.A. Shchukin, N.N. Ledentsov, and D. Bimberg, *Epitaxy of Nanostructures* (Springer, Berlin, 2003).
- [3] D. Pachinger, H. Groiss, M. Teuchtmann, G. Hesser, and F. Schäffler, *Appl. Phys. Lett.* **98**, 223104 (2011).
- [4] T. Markurt, L. Lymparakis, J. Neugebauer, P. Drechsel, P. Stauss, T. Schulz, T. Remmele, V. Grillo, E. Rotunno, and M. Albrecht, *Phys. Rev. Lett.* **110**, 036103 (2013).
- [5] N.V. Medhekar, V. Hegadekatte, and V.B. Shenoy, *Phys. Rev. Lett.* **100**, 106104 (2008); X.B. Niu, G.B. Stringfellow, and F. Liu, *Phys. Rev. Lett.* **107**, 076101 (2011).
- [6] M.S. Levine, A.A. Golovin, S.H. Davis, and P.W. Voorhees, *Phys. Rev. B* **75**, 205312 (2007); D. Pontoni, K.J. Alvine, A. Checco, O. Gang, B.M. Ocko, and P.S. Pershan, *Phys. Rev. Lett.* **102**, 016101 (2009).
- [7] O. Pierre-Louis, A. Chame, and Y. Saito, *Phys. Rev. Lett.* **103**, 195501 (2009).
- [8] T.V. Savina, P.W. Voorhees, and S.H. Davis, *J. Appl. Phys.* **96**, 3127 (2004); D. Schebarchov, Sh.C. Hendy, E. Ertekin, and J.C. Grossman, *Phys. Rev. Lett.* **107**, 185503 (2011).
- [9] V.A. Shchukin, N.N. Ledentsov, P.S. Kop'ev, and D. Bimberg, *Phys. Rev. Lett.* **75**, 2968 (1995).
- [10] I.L. Daruka and A.-L. Barabási, *Phys. Rev. Lett.* **79**, 3708 (1997); G. Medeiros-Ribeiro, A.M. Bratkovski, T.I. Kamins, D.A.A. Ohlberg, and R.S. Williams, *Science* **279**, 353 (1998).
- [11] D.E. Jesson, G. Chen, K.M. Chen, and S.J. Pennycook, *Phys. Rev. Lett.* **80**, 5156 (1998).
- [12] M. Berti, A.V. Drigo, G. Rossetto, and G. Torzo, *J. Vac. Sci. Technol. B* **15**, 1794 (1997); A. Urbanczyk and R. Nötzel, *J. Cryst. Growth* **341**, 24 (2012).
- [13] Y. Shim and J.G. Amar, *Phys. Rev. Lett.* **108**, 076102 (2012).
- [14] R.E. Rudd, G.A.D. Briggs, A.P. Sutton, G. Medeiros-Ribeiro, and R.S. Williams, *Phys. Rev. Lett.* **90**, 146101 (2003).
- [15] N.N. Ledentsov, V.A. Shchukin, D. Bimberg, V.M. Ustinov, N.A. Cherkashin, Yu.G. Musikhin, B.V. Volovik, G.E. Cirlin, and Zh.I. Alferov, *Semicond. Sci. Technol.* **16**, 502 (2001).
- [16] J. Tersoff, *Phys. Rev. B* **43**, 9377 (1991).
- [17] L.G. Wang, P. Kratzer, M. Scheffler, and N. Moll, *Phys. Rev. Lett.* **82**, 4042 (1999).
- [18] M.J. Beck, A. van de Walle, and M. Asta, *Phys. Rev. B* **70**, 205337 (2004).
- [19] G.B. Stringfellow, *J. Appl. Phys.* **54**, 404 (1983).
- [20] To find the minimum of the energy (4), we first express the island size  $L$  in terms of the fraction  $q \leq 1 - \nu$  of the surface covered by the 3D islands of  $B$ ,  $L = 6a \cot \partial_B N_2 q^{-1}$ . Second, we seek the minimum of Eq. (4) with respect to  $\nu$  and then with respect to  $q$ , at fixed  $N_1$  and  $N_2$ . Finally, we run the remaining function over all possible  $N_1$  and  $N_2$  with the step 0.001 and thus find the sought values.
- [21] M. Meixner and E. Schöll, *Phys. Rev. B* **67**, 121202 (2003).
- [22] S. Mirbt, N. Moll, A. Kley, and J.D. Joannopoulos, *Surf. Sci.* **422**, L177 (1999).
- [23] N.E. Christensen, *Solid State Commun.* **68**, 959 (1988).
- [24] It is worth noting that some intermixing may occur between Al and In that would require considering the free energy by adding an entropy term to Eqs. (2) and (4). However, as a strong driving force to phase separation is known for the InAs-AlAs system, which manifests itself, e.g., in the growth of an InAlAs alloy film [e.g., S.W. Jun, T.-Y. Seong, J.H. Lee, and B. Lee, *Appl. Phys. Lett.* **68**, 3443 (1996)], one expects that the results of our consideration will only slightly alter, and the WL will contain Al-rich domains (with a small fraction of In) and In-rich domains (with a small fraction of Al), and the component lattice mismatched to the substrate (in this case, InAs) will predominantly be driven to 3D islands [5]. Thus, the major effect of an earlier onset of 3D islands stimulated by the AlAs deposition will persist.
- [25] The deposition of InAs on AlAs or GaAlAs(100) shifts the onset of 3D islands to thicker critical WLs due to a stronger InAs wetting on AlAs-enriched surfaces: P. Ballet, J.B. Smathers, H. Yang, C.L. Workman, and G.J. Salamo, *J. Appl. Phys.* **90**, 481 (2001).
- [26] A.F. Tsatsul'nikov, A.R. Kovsh, A.E. Zhukov, Yu. M. Shernyakov, Yu. G. Musikhin, V.M. Ustinov, N.A. Bert, P.S. Kop'ev, Zh.I. Alferov, A.M. Mintairov, J.L. Merz, N.N. Ledentsov, and D. Bimberg, *J. Appl. Phys.* **88**, 6272 (2000).
- [27] A high density ( $0.9 \times 10^{11} \text{ cm}^{-2}$ ) of large size submonolayer InAs islands ( $\sim 15 \text{ nm}$ ) was observed for  $\text{Al}_{0.6}\text{Ga}_{0.4}\text{As}$  spacers, while the density was much lower ( $0.08 \times 10^{11} \text{ cm}^{-2}$ ) for GaAs spacers, where the nonwetting effects are much weaker: A.F. Tsatsul'nikov, B.V. Volovik, N.N. Ledentsov, M.V. Maximov, A. Yu. Egorov, A.R. Kovsh, V.M. Ustinov, A.E. Zhukov, P.S. Kop'ev, Zh.I. Alferov, I.A. Kozin, M.V. Belousov, I.P. Soshnikov, P. Werner, D. Litvinov, U. Fischer, A. Rosenauer, and D. Gerthsen, *J. Electron. Mater.* **28**, 537 (1999).
- [28] If materials  $B$  and  $C$  are deposited together, the trend to phase separation favors, at the very initial stage of the deposition, the formation of domains of  $B$  and domains of  $C$ , each having an interface with substrate  $A$ . If  $C$  forms, due to growth kinetics, locally extended two-dimensional (2D) islands on  $A$ , then deposition of  $B$  on top of  $C$  proceeds in a 2D mode up to a larger thickness than in a  $B/A$  system, due to the stronger wetting effects of  $B$  on  $C$ , and the formation of 3D islands is thus relatively suppressed. As opposite, if 2D domains of  $B$  form locally on  $A$ , the subsequent deposition of  $C$  on top will stimulate formation of 3D islands of  $B$  as discussed above. However, the transformation may be affected by the finite size of 2D domains of  $B$  and more complex growth kinetics. Thus, in general, one may conclude that the formation of 3D islands, for nominally the same deposited amounts of  $B$  and  $C$ , should be less pronounced in the case of the simultaneous deposition of both materials.